*J. Indian Soc. Coastal Agric. Res. 42(1):14-23(2024) https://doi.org/10.54894/JISCAR.42.1.2024.147381*

# Performance of MODIS-Landsat Blending of Vegetation Indices in the Coastal Zone of Ganges Delta

J.L. PEÑA - ARANCIBIA* and Y. YU

Commonwealth Scientific and Industrial Research Organisation (CSIRO), Canberra, ACT - 2601, Australia

Received: 12.01.2024 Accepted: 20.03.2024

**Blending of temporal high-frequency-low-spatial resolution MODIS with temporal low-frequency-high-spatial resolution Landsat satellite imagery enhances the frequency and resolution of spatial data, thus enabling continuous monitoring of dynamic and rapidly changing environmental conditions. Blending can be particularly useful in areas with high cloud cover, such as during the monsoon season in the coastal zone of the Ganges Brahmaputra Delta (CZGBD). In this study, MODIS - Landsat blending of reflectance-derived remote sensing indices is trialled and evaluated in the CZGBD. The Sub-pixel class fraction change information Flexible Spatiotemporal DAta Fusion (SFSDAF) algorithm is used to obtain gap free 30 m and 16 - day frequency vegetation, salinity and water indices for the entire CZGBD. Pixels obtained through blending were compared to the observed pixels (*i.e.*, not contaminated by clouds to evaluate the accuracy of SFSDAF). Results during the 'dry' months (October to March) had a combined mean coefficient of determination, $R^2$ = 0.65 and mean root squared error, RMSE = 0.09 for vegetation indices, whereas the results during the 'wet' months (April to September) had a combined mean $R^2$ = 0.33 and mean RMSE = 0.12. The reduced accuracy of the blending during the monsoon months showcases the effects of cloudy conditions. Results for salinity and water indices showed similar behaviour as the vegetation indices, influenced by the cloudy monsoon season. The main cause of low accuracy during the 'wet' months is the paucity of data to perform the blending, even at the daily MODIS frequency. In addition, remote sensing indices with equations that normalised the range (generally between - 1 and 1) had better results when compared to remote sensing indices that had less constrained ranges.**

(***Key words:*** *Image processing, Monitoring, Remote sensing, Vegetation indices, Satellites)*

Coastal river deltas are hotspots of global change, governed not only by the natural movement of river and tidal water, but also by increasing anthropogenic modification (Hagenlocher *et al.*, 2018). The coastal zone of the Ganges - Brahmaputra Delta (CZGBD, Fig. 1), the largest in the world (1.72 million km$^2$), holds exceptional importance for its biodiversity, rich agricultural lands, ecosystem services and cultural significance for its more than 15 million inhabitants (Mainuddin *et al.,* 2021; Rahman *et al.,* 2022). The CZGBD is experiencing increasing extreme weather events (Swapna *et al.,* 2022) leading to floods, cyclonic storms, storm surges and salinity intrusion. Concurrently, intense anthropogenic modification (*i.e.,* land use change and development of infrastructure such as roads, dikes and embankments) has changed some of the naturally occurring dynamics in the CZGBD.

Changing weather patterns, climate change-induced sea level rise, and population exposure increase the risk for the CZGBD inhabitants and its life support systems (Mainuddin *et al.,* 2019; Szabo *et al.,* 2016).

In recent decades, monitoring environmental change at the regional scale has been facilitated by satellite remote sensing (RS). As a hotspot for global change, RS can underpin environmental and resource management in the CZGBD, including monitoring of natural hazards (cyclones, droughts, floods and land subsidence), biodiversity threats (deforestation, vegetation health and water quality), land use change (agricultural practices, urbanization, and other human-induced alterations), the water balance (evapotranspiration, surface and groundwater water storage and rainfall) and food security (crop mapping and crop yield estimation). Optical RS data from satellites such as Landsat and Sentinel-2 have been used for regional biophysical assessments and monitoring in the CZGBD (Ghosh *et al.,* 2023; Nanda *et*

**Corresponding author*: E-mail: jorge.penaarancibia@csiro.au

*al.,* 2023; Raut *et al.,* 2015; Shimu *et al.,* 2019; Sunny *et al.,* 2022). However, prevalent cloud cover, particularly during the monsoon months (June to October), results in gaps in satellite imagery which affects optical RS-based assessment and monitoring. The blending of optical satellite imagery characterized by 'low spatial resolution-high temporal frequency' - capturing less detail but taken at frequent intervals - with 'high spatial resolution-low temporal frequency' images - providing more detail but captured less often - has emerged as a widely adopted technique to reduce data gaps (Gao *et al.,* 2006). Several approaches, each with their strengths and weaknesses, have been successfully used to fill gaps in imagery using blending. In this research, the accuracy of blending RS indices (vegetation, salinity and water detection) Moderate Resolution Imaging Spectroradiometer (MODIS, Strahler *et al.,* 1999) imagery at daily frequency and 500 m spatial resolution with Landsat 5, 7 and 8 (Wulder *et al.,* 2016) imagery at 16-day resolution (or 8-day when two satellites are available) and 30 m resolution for the entire CZGBD is assessed. The blended 16-day frequency and 30 m spatial resolution RS indices can provide a gap free continuous time series, both during the 'wet' months (April to September) and 'dry' months. (October to March) and thus enhance RS-based assessment and monitoring.

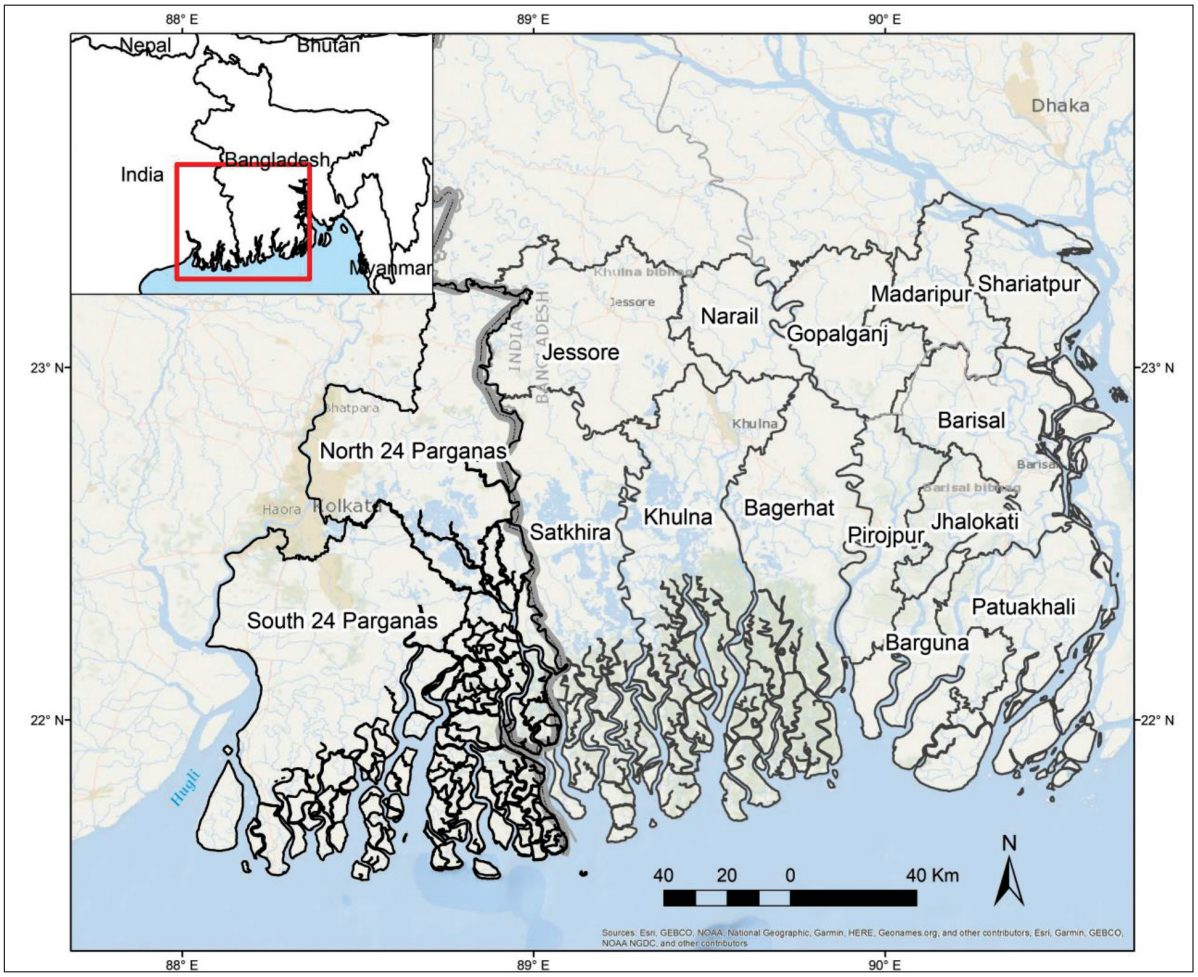


***Fig. 1.*** *Study area in the coastal zone of Bangladesh and West Bengal (India) showing district boundaries (black lines) and associated names*

## MATERIALS AND METHODS

### Satellite imagery

A total of 2637 Landsat 5, 7 and 8 cloud free surface reflectance imagery were pre-processed and downloaded from Google Earth Engine (Gorelick *et al.,* 2017), encompassing February 2000 to May 2022. In addition, surface reflectance imagery from the Nadir Bidirectional Reflectance Distribution Function Adjusted Reflectance (NBAR) product from the Moderate Resolution Imaging Spectroradiometer (MODIS, Strahler *et al.,* 1999) satellite (MCD43A4 V6.1) were also sourced from Google Earth Engine. MCD43A4 V6.1 is a daily product based on a 16-day retrieval period, with the image's date occurring on the 9th day. This product combines data from both the Terra and Aqua spacecrafts, choosing the best representative pixel from the 16-day period.

### Image completeness

All the available CZGBD satellite imagery for both Landsat and MODIS from GEE were composited to overlapping 16-day periods. Subsequently, gaps due to cloud cover and missing data were assessed at the monthly frequency (*i.e.,* wherever month data of the 16-day composite belonged to), reporting image completeness in percentage terms.

### Remote sensing indices

Rather than blending satellite reflectance data, the approach of obtaining RS indices first and then blending these was chosen because of its better performance than blending reflectances and then computing indices (Jarihani *et al.,* 2014). The RS indices used in this research are summarised in Table 1. These indices are routinely used for environmental assessments and monitoring, including vegetation, salinity, and water indices. The indices were chosen based on their formulations and bands used in their calculation, trying to incorporate most bands from both Landsat and MODIS sensors and normalised indices (like the Normalised Difference Vegetation Index, NDVI) and additive indices (like the Brightness Index, BI).

***Table 1.*** *Summary of satellite indices used in this research*

| Index | Formula | Reference |
|---|---|---|
| Normalised Difference Vegetation Index | $NDVI = \frac{NIR - Red}{NIR + Red}$ | Kriegler *et al.* (1969) |
| Enhanced Vegetation Index | $EVI = 2.5 \times \frac{NIR - Red}{(NIR + 6 \times Red - 7.5 \times Blue) + 1}$ | Huete *et al.* (2002) |
| Global Vegetation Moisture Index | $GVMI = 2.5 \times \frac{(NIR - 0.1) + (SWIR1 - 0.02)}{(NIR + 0.1) + (SWIR1 + 0.02)}$ | Ceccato *et al.* (2002) |
| Brightness Index | $BI = \sqrt{Red^2 + NIR^2}$ | Khan *et al.* (2005) |
| Vegetation Soil Salinity Index | $VSSI = 2 \times Green - 5 \times (Red + NIR)$ | Nguyen *et al.* (2020) |
| Automatic Water Extraction Index with shadow | $AWEI_{shadow} = Blue + 2.5 \times Green - 1.5 \times (NIR + SWIR1) - 0.25 \times SWIR2$ | Feyisa *et al.* (2014) |

### MODIS-Landsat blending

The sub-pixel class fraction change information Flexible Spatiotemporal DAta Fusion (SFSDAF) method (Li *et al.,* 2020) was used in the analysis. SFSDAF only requires one pair of gap free MODIS and Landsat images 'before prediction' and one gap free MODIS image 'at prediction' to produce a 'Landsat like' gap free image 'at prediction'. SFSDAF has the ability of detecting gradual (*i.e.,* phenological) or abrupt (*e.g.,* floods) land cover changes (Li *et al.,* 2020). When predicting the 'Landsat like' image, the final image retains the observed pixels (*i.e.,* the original Landsat image at prediction) and only the gaps are replaced with predicted pixels. A flowchart of this process is shown in Fig. 2. The coefficient of determination ($R^2$) and root-mean-squared error (RMSE) of the predicted pixels (*i.e.,* 'Landsat like' image) versus the observed pixels were used as goodness-of-fit metrics.

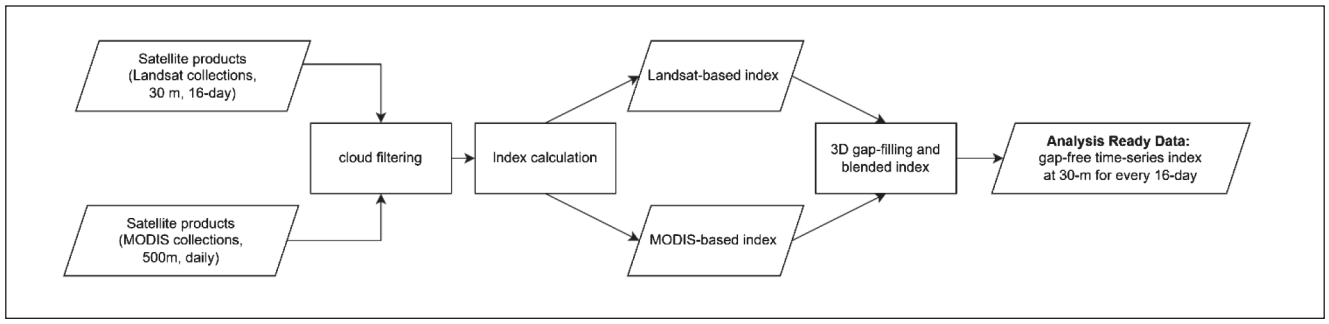


***Fig. 2.*** *Blending workflow*

Firstly, RS indices were computed from the cloud free Landsat imagery. Secondly, a 16-day composite (including all Landsat 5, Landsat 7 and Landsat 8 imagery) was produced for each index by taking the mean of all cloud free imagery within the 16-day period (starting on 1 January each year until 18 December, with this last period composite including imagery until January 3 to complete the 16 days). Thirdly and finally, every 16-day Landsat composite that was gap free (*i.e.,* clear sky conditions or completed through the compositing procedure) was used in the blending as 'before prediction' images. The procedure ensured not to have 'before prediction' images occurring many months before 'at prediction' images, a 3-month threshold was enforced as well as a requirement that the 'before prediction' image did not straddle into another season (*i.e.,* from the 'wet' to the 'dry' and *vice versa*) as vegetation phenology (and their reflectance, either natural vegetation or crops) and other biophysical processes (*e.g.,* inundation) responds to this seasonality.

A similar procedure was followed for MCD43A4 V6.1 imagery. Because of the prevailing cloud cover during the monsoon months, even the daily MCD43A4 V6.1 imagery had gaps. These gaps were filled using the method of Wang *et al.* (2012) which performs a three-dimensional interpolation (*i.e.,* both in space and time) and was previously successfully assessed in Bangladesh (Peña-Arancibia *et al.,* 2021).

## RESULTS AND DISCUSSION

### Image completeness

Both MCD43A4 V6.1 and Landsat imagery were assessed in terms of completeness at the monthly frequency from January 2000 to May 2022. MCD43A4 V6.1 was available from 18 February 2000 to 24 May 2022. Until May 2002, when the Aqua satellite was launched, only the Terra satellite and corresponding imagery was available. Fig. 3a shows the image completeness for MCD43A4 V6.1, with contrasting results for the 'wet' months (April to September) and 'dry' months (October to March). Fig. 3a shows the influence of the cloudy monsoon months, with image completeness generally < 40% during the peak monsoon months (June to August).

Landsat 5 imagery was available from 3 January 2000 to 11 November 2011; Landsat 7 imagery was available from 3 February 2000 to 6 April 2022; and Landsat 8 imagery was available from 12 April 2013 to 26 May 2022. In late May 2003, the Scan Line Corrector (SLC) failed in Landsat 7, resulting in a two - month gap in image acquisition; subsequently, the images acquired had ~20% data gaps (Goward *et al.,* 2006). In addition, not all Landsat images - particularly for Landsat 5 TM - that were historically acquired are currently part of the consolidated Landsat Global Archive Consolidation (LGAC, Wulder *et al.,* 2016). The causes of the low (< 60%) imagery completeness from 2000 to 2004 showcases this issue. Landsat imagery completeness improves for the months outside of the peak monsoon from 2005, with completeness > 60% in most months, visibly so after Landsat 8 imagery was available in 2013. A summary of image completeness for both 'wet' months (April to September) and 'dry' months. (October to March) is shown in Table 2.

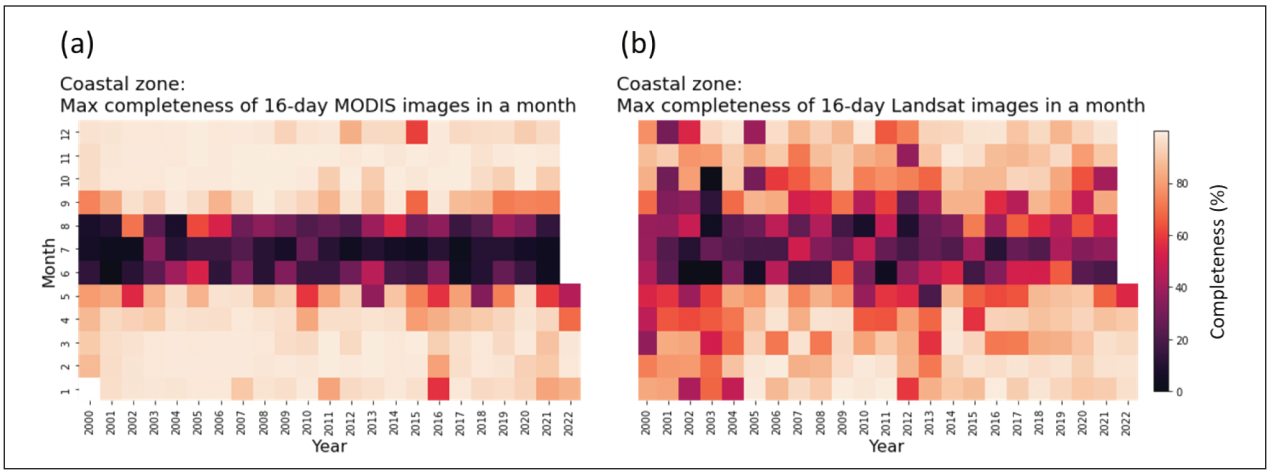


***Fig. 3.*** *Percentage image completeness for MODIS and Landsat 16 - day composites from January 2000 to May 2020 (with darker tones in the red hue denoting more missing data)*

***Table 2.*** *Summary of image completeness per season, 'wet' months (April to September) and 'dry' months. (October to March)*

| Dataset | Season | 2000-2010 | 2010-2020 |
|---|---|---|---|
| Landsat | Wet | 35.61% | 41.67% |
| Landsat | Dry | 69.66% | 81.14% |
| MODIS | Wet | 47.99% | 43.93% |
| MODIS | Dry | 97.11% | 93.46% |

**MODIS-Landsat blending**

Blending was implemented to obtain a 16-day frequency 30 m spatial resolution time series. A total of 420 16-day composites out of 520 required blending. An example of an image (a pseudo - RGB from the NDVI, EVI and GVMI vegetation indices, see Table 1) for the entire CZGBD on 3 February 2007 with gaps and after MODIS - Landsat blending is shown in Fig. 4. The image with gaps has been masked for clouds, a part of the image missing (as no Landsat images were available for the 16-day composite), and the effects of Landsat 7's SCL failure are shown as contiguous lines with missing data. At a qualitative visual inspection, the blended image shows no noticeable artifacts. In terms of vegetation indices (Table 1) the blended image had mean simulated NDVI, EVI and GVMI of 0.33, 0.24 and 0.30, respectively, compared to the mean observed NDVI, EVI and GVMI of 0.45, 0.28 and 0.29. The $R^2$ for NDVI, EVI, and GVMI in the image were 0.58, 0.76 and 0.67, respectively, and the RMSE were 0.07, 0.04 and 0.07.

The overall results for the vegetation, salinity and water indices from Table 1 are summarised in Fig. 5.

The blending results in Fig. 5 showcase differences for each index and for the month of year. The median $R^2$, generally > 0.6 for all indices during the dry months (October to March), generally drops < 0.3 during the wet months (April to September). Normalized indices such as NDVI, EVI and GVMI, whose range in this research was bounded from 0 to 1, have a similar $R^2$ pattern in each month, with GVMI performing poorer than both NDVI and EVI. Interestingly, AWEIsh blended results show median $R^2$ > 0.5 for all months. AWEIsh is an additive index (Table 1) using bands in the visible and shortwave infrared spectrum. Both salinity indices BI and VSSI had a similar overall pattern in terms of median $R^2$ (*i.e.,* better during the dry months than during the wet months), however the variability was larger (note the shape of the violin plots in Fig. 5 showcasing the data distribution). In addition, blended BI systematically underestimated observed BI, whereas

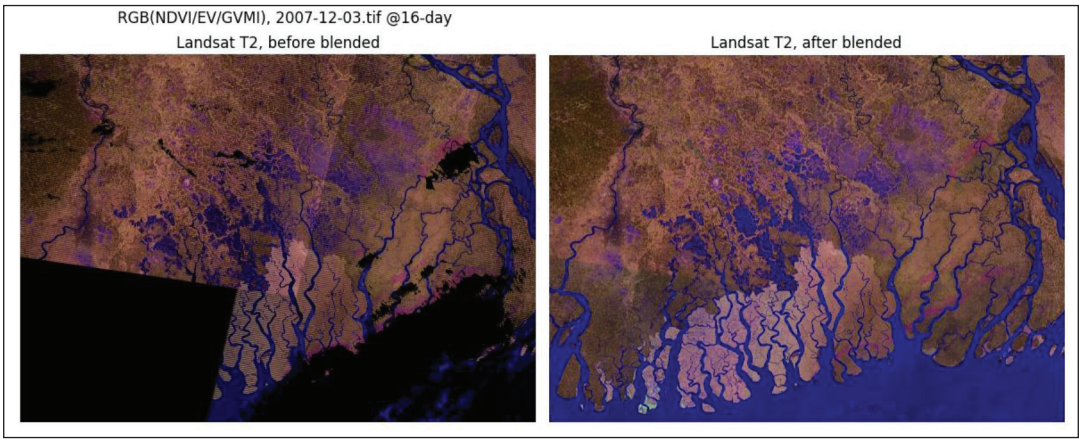


***Fig. 4.*** *Example of an image for 2007-12-03 with gaps (in black) and blended, shown as a pseudo RGB composite of NDVI/EVI/GVMI. From left to right, the first panel shows an image with gaps (including clouds, a portion of the image missing, and the effects of Landsat-7's SCL failure shown as contiguous lines with missing data), the second panel shows the Landsat blended image with gaps filled*

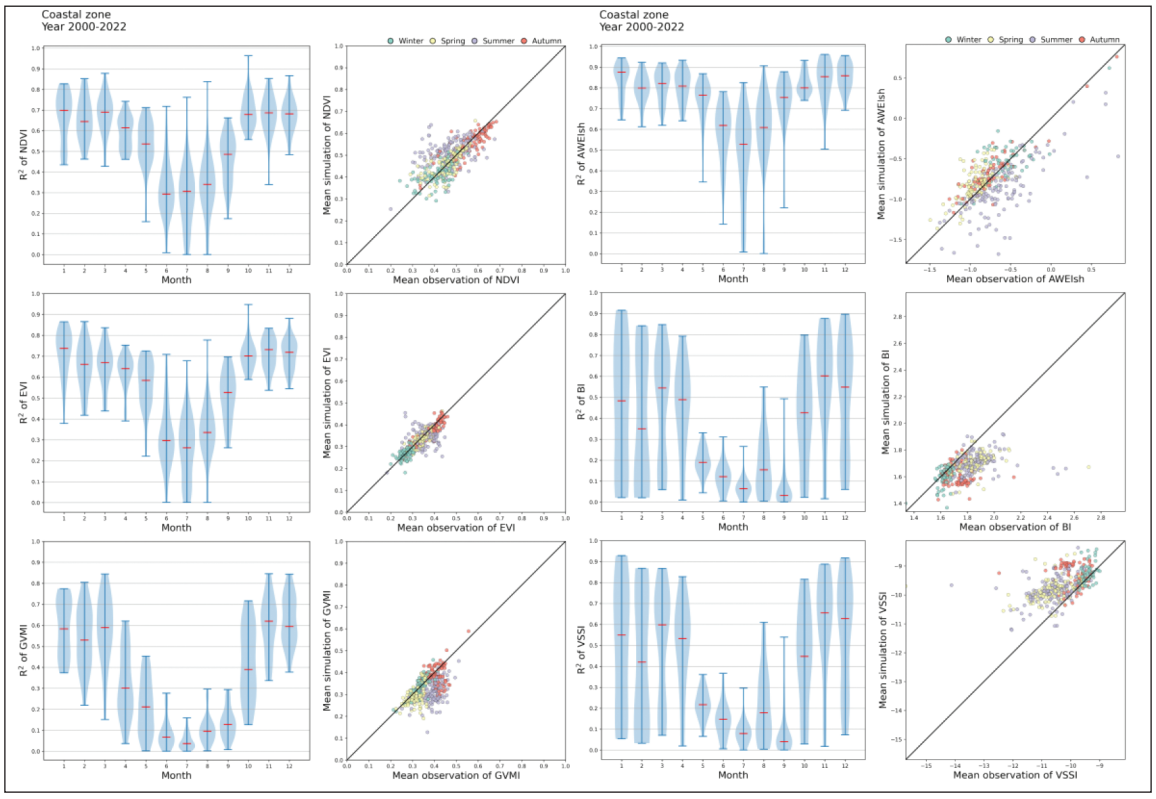


***Fig. 5.*** *Blending accuracy summary for remote sensing indices. The left panel shows coefficient of determination ($R^2$) violin plots for all indices in each month (1 for January, 2 for February, etc.) for all analysis years combined. The right panel shows a scatterplot between the mean and predicted remote sensing indices values*

***Table 3.*** *Summary of blending results for all remote sensing indices. Results are disaggregated into dry (October to March) and wet months (April to September).*

| Season | Index | # images | Mean observed | Mean simulated | Mean $R^2$ | Mean RMSE |
|---|---|---|---|---|---|---|
| Dry | NDVI | 170 | 0.47 | 0.47 | 0.67 | 0.09 |
| Dry | EVI | 170 | 0.31 | 0.31 | 0.69 | 0.07 |
| Dry | GVMI | 170 | 0.34 | 0.35 | 0.56 | 0.10 |
| Dry | AWEIsh | 114 | -0.71 | -0.61 | 0.82 | 0.34 |
| Dry | BI | 125 | 1.67 | 1.63 | 0.47 | 0.23 |
| Dry | VSSI | 125 | -9.64 | -9.42 | 0.51 | 1.34 |
| Wet | NDVI | 250 | 0.48 | 0.50 | 0.42 | 0.13 |
| Wet | EVI | 250 | 0.36 | 0.35 | 0.43 | 0.10 |
| Wet | GVMI | 250 | 0.37 | 0.31 | 0.15 | 0.13 |
| Wet | AWEIsh | 245 | -0.74 | -0.84 | 0.65 | 0.52 |
| Wet | BI | 248 | 1.85 | 1.68 | 0.18 | 0.35 |
| Wet | VSSI | 248 | -10.61 | -9.73 | 0.20 | 2.04 |

blended VSSI systematically overestimated observed VSSI. The vegetation and water indices did not show these biases. A summary of metrics for the dry and wet months for each index is shown in Table 3.

It is noted that the SFSDAF method was developed for blending reflectances and not RS indices (Li *et al.,* 2020), which may partly explain why the blending for normalised indices (*i.e.,* NDVI, EVI and GVMI) generally performs better than additive ones, with the exception of AWEIsh, but whose range is also generally from -1 to 1 (Fisher *et al.,* 2016).

MODIS-Landsat blending using the SFSDAF method has been successfully implemented in the CZGBD, but accuracy metrics during the monsoon months (April to October) still show the difficulties due to data paucity because of cloudy conditions. Including other more recent optical data such as the 5-day frequency and 10 - 20 m spatial resolution like Sentinel - 2 (Drusch *et al.,* 2012) and the daily 500 - 1000 m Visible Infrared Imaging Radiometer Suite (VIIRS, Welsch *et al.,* 2001) in the 16-day composites may improve the data availability and therefore the blending in SFSDAF or other blending algorithms. If blending reflectances, these may need to be harmonised for better results to be achieved (*e.g.,* Roy *et al.,* 2016). It is noted though that even the daily MODIS MCD43A4 V6.1 product has low image completeness during the monsoon months, as prevailing cloud cover may affect the larger 500 m pixels more pervasively than for Landsat (Melchiorre *et al.,* 2020).

## CONCLUSION

In the last two decades, remote sensing (RS) has prominently emerged as a cost - effective and practical method for environmental and resource assessment and monitoring at the regional scale. In this research, blending of optical RS data was implemented in the coastal zone of the Ganges - Brahmaputra Delta (CZGBD) to overcome data paucity, particularly during the cloudy monsoon months (April to October). MODIS - Landsat blending using the SFSDAF method was trialled for vegetation, salinity and water RS indices. A 16-day temporal frequency and native Landsat 30 m spatial resolution was chosen for the blending. SFSDAF was more successful in blending indices whose ranges varied mostly from 0 to 1, including the vegetation indices NDVI, EVI, GVMI and the water index AWEIsh.

The goodness-of-fit metrics were reasonable (combined vegetation indices mean $R^2$ = 0.65 and mean RMSE = 0.09) during the dry months (October to March) but deteriorated (mean $R^2$ = 0.33 and mean RMSE = 0.12) during the wet months (April to September) highlighting the difficulties in overcoming the prevailing cloud cover in the CZGBD, particularly during the monsoon months. Results for salinity and water indices showed similar behavior as the vegetation indices, influenced by the cloudy monsoon season.

The CZGBD is a hotspot for global change and RS plays a pivotal role in regional resource assessments and monitoring. Techniques like blending can help overcome data gaps and generate gap free time series that can be used for several purposes (*e.g.,* land use change, vegetation health, water balance and crop mapping). However, areas with prevailing cloud cover like the CZGBD during the monsoon, will still face challenges due to the lack of sufficient 'clear sky' conditions. This may be overcome by integrating additional optical RS data.

## CONFLICTS OF INTEREST

There authors declare no conflicts of interest.

## ACKNOWLEDGEMENT

This research was funded by the Australian Centre for International Agricultural Research (ACIAR) and Krishi Gobeshona Foundation (KGF) of Bangladesh under the project "Cropping system intensification in the salt-affected coastal zone of Bangladesh and West Bengal, India (CSI4CZ) Phase II". The authors thank an anonymous reviewer for providing helpful comments, and Dr. Tashi Dorjee Lama, Editor in Chief, for handling the peer-review-process.

## REFERENCES

Ceccato, P., Flasse, S. and Gregoire, J.M. (2002). Designing a spectral index to estimate vegetation water content from remote sensing data - Part 2. Validation and applications. *Remote Sensing of Environment* **82**(2): 198-207. https://doi.org/10.1016/S0034-4257(02)00036-6.

Drusch, M., Del Bello, U., Carlier, S., Colin, O., Fernandez, V., Gascon, F., Hoersch, B., Isola, C., Laberinti, P., Martimort, P., Meygret, A., Spoto, F., Sy, O., Marchese, F. and Bargellini, P. (2012). Sentinel-2: ESA's optical high-resolution mission for gmes operational services. *Remote Sensing of Environment* **120**: 25-36. https://doi.org/10.1016/j.rse.2011.11.026.

Feyisa, G.L., Meilby, H., Fensholt, R. and Proud, S.R. (2014). Automated Water extraction index: A new technique for surface water mapping using Landsat imagery. *Remote Sensing of Environment* **140**: 23-35. https://doi.org/10.1016/j.rse.2013.08.029.

Fisher, A., Flood, N. and Danaher, T. (2016). Comparing Landsat water index methods for automated water classification in eastern Australia. *Remote Sensing of Environment* **175**: 167-182. https://doi.org/10.1016/j.rse.2015.12.055.

Gao, F., Masek, J., Schwaller, M. and Hall, F. (2006). On the blending of the Landsat and MODIS surface reflectance: Predicting daily Landsat surface reflectance. *Ieee Transactions on Geoscience and Remote Sensing* **44**(8): 2207-2218. https://doi.org/10.1109/Tgrs.2006.872081.

Ghosh, A., Nanda, M. K., Sarkar, D., Sarkar, S., Brahmachari, K. and Mainuddin, M. (2023). *Kharif* rice growth and area monitoring in Gosaba CD block of Indian Sundarbans region using multi - temporal dual - pol SAR data. *Environment, Development and Sustainability.* https://doi.org/10.1007/s10668-023-04138-4.

Gorelick, N., Hancher, M., Dixon, M., Ilyushchenko, S., Thau, D. and Moore, R. (2017). Google Earth Engine: Planetary-scale geospatial analysis for everyone. *Remote Sensing of Environment* **202**: 18-27. https://doi.org/10.1016/j.rse.2017.06.031.

Goward, S., Arvidson, T., Williams, D., Faundeen, J., Irons, J., and Franks, S. (2006). Historical record of Landsat global coverage: Mission operations, NSLRSDA, and international cooperator stations. *Photogrammetric Engineering and Remote Sensing* **72**(10): 1155 - 1169. https://doi.org/10.14358/Pers.72.10.1155.

Hagenlocher, M., Renaud, F.G., Haas, S. and Sebesvari, Z. (2018). Vulnerability and risk of deltaic social-ecological systems exposed to multiple hazards. *Science of the Total Environment* **631-632**: 71-80.

https://doi.org/10.1016/j.scitotenv.2018.03.013.

Huete, A., Didan, K., Miura, T., Rodriguez, E.P., Gao, X. and Ferreira, L.G. (2002). Overview of the radiometric and biophysical performance of the MODIS vegetation indices. *Remote Sensing of Environment* **83**(1-2): 195-213. https://doi.org/10.1016/S0034-4257(02)00096-2.

Jarihani, A.A., McVicar, T.R., Van Niel, T.G., Emelyanova, I.V., Callow, J.N. and Johansen, K. (2014). Blending Landsat and MODIS Data to generate multispectral indices: A comparison of "Index-then-Blend" and "Blend-then-Index" approaches. *Remote Sensing* **6**(10): 9213-9238. https://doi.org/10.3390/rs6109213.

Khan, N.M., Rastoskuev, V.V., Sato, Y. and Shiozawa, S. (2005). Assessment of hydrosaline land degradation by using a simple approach of remote sensing indicators. *Agricultural Water Management* **77**(1-3): 96-109.

Kriegler, F., Malila, W., Nalepka, R. and Richardson, W. (1969). Preprocessing transformations and their effect on multispectral recognition, Proceedings 6th International Symposium on *Remote sensing of environment,* University of Michigan, Ann Arbor, MI, USA. pp 97-131.

Li, X.D., Foody, G.M., Boyd, D.S., Ge, Y., Zhang, Y.H., Du, Y. and Ling, F. (2020). SFSDAF: An enhanced FSDAF that incorporates sub-pixel class fraction change information for spatio-temporal image fusion. *Remote Sensing of Environment* **237**. https://doi.org/10.1016/j.rse.2019.111537.

Mainuddin, M., Bell, R., Gaydon, D., Kirby, M., Barrett-Lennard, E., Glover, M., Akanda, M.A., Maji, B., Ali, A., Brahmachari, K., Maniruzzaman, M., Aziz, M.A., Burman, D., Biswas, J.C., Rahman, M.M. and Sarangi, S.K. (2019). An overview of the Ganges coastal zone: Climate, hydrology, land use, and vulnerability. *Journal of the Indian Society of Coastal Agricultural Research* **37**(2): 1-11.

Mainuddin, M., Karim, F., Gaydon, D.S. and Kirby, J.M. (2021). Impact of climate change and management strategies on water and salt balance of the polders and islands in the Ganges delta. *Scientific Reports* **11**(1). https://doi.org/10.1038/s41598-021-86206-1.

Melchiorre, A., Boschetti, L. and Roy, D.P. (2020). Global evaluation of the suitability of MODIS-Terra detected cloud cover as a proxy for Landsat 7 cloud conditions. *Remote Sensing* **12**(2). https://doi.org/10.3390/rs12020202.

Nanda, M.K., Ghosh, A., Sarkar, D., Sarkar, S., Brahmachari, K., Ray, K., Goswami, R. and Mainuddin, M. (2023). Assessing the seasonal crop acreage in the Ganges Delta using multi-temporal Sentinel-2 data: A case study in Gosaba CD Block. *Journal of the Indian Society of Coastal Agricultural Research* **41**(1): 24-40. https://doi.org/10.54894/JISCAR.41.1.2023.129996.

Nguyen, K.A., Liou, Y.A., Tran, H.P., Hoang, P.P. and Nguyen, T.H. (2020). Soil salinity assessment by using near-infrared channel and Vegetation Soil Salinity Index derived from Landsat 8 OLI data: A case study in the Tra Vinh Province, Mekong Delta, Vietnam. *Progress in Earth and Planetary Science* **7**(1): 1. https://doi.org/10.1186/s40645-019-0311-0.

Peña-Arancibia, J. L., Golam Mahboob, M., Islam, T., Mainuddin, M., Yu, Y., Ahmad, M.D., Ibn Murad, K., Saha, K., Hossain, A., Moniruzzaman, M., Ticehurst, C. and Kong, D.D. (2021). The green revolution from space: Mapping the historic dynamics of main rice types in one of the world's food bowls. *Remote Sensing Applications: Society and Environment* **21**: 100460. https://doi.org/10.1016/j.rsase.2020.100460.

Rahman, M.M., Haque, A., Nicholls, R.J., Darby, S.E., Urmi, M.T., Dustegir, M.M., Dunn, F.E., Tahsin, A., Razzaque, S., Horsburgh, K. and Haque, M.A. (2022). Sustainability of the coastal zone of the Ganges-Brahmaputra-Meghna delta under climatic and anthropogenic stresses. *Science of the Total Environment* **829**. https://doi.org/10.1016/j.scitotenv.2022.154547.

Roy, D.P., Kovalskyy, V., Zhang, H.K., Vermote, E.F., Yan, L., Kumar, S.S. and Egorov, A. (2016). Characterization of Landsat-7 to Landsat-8 reflective wavelength and normalized difference vegetation index continuity. *Remote Sensing of Environment* **185**: 57-70. https://doi.org/10.1016/j.rse.2015.12.024.

Shimu, S.A., Aktar, M., Ibn Afjal, M., Nitu, A.M., Uddin, M.P. and Al Mamun, M. (2019). NDVI based change detection in Sundarban mangrove forest using remote sensing data, 4th International Conference on *Electrical information and communication technology (EICT),* Khulna, Bangladesh. https://doi.org/10.1109/eict48899.2019.9068819.

Raut, S., Buddheswar, M., Subrata, M. and Lama, T. D. (2015). Study of vegetation index, land use and irrigation scheduling efficiency as affected by soil salinity in different blocks of coastal West Bengal using remote sensing and GIS. *Journal of the Indian Society of Coastal Agricultural Research* **33**(2): 1-6.

Strahler, A.H., Lucht, W., Schaaf, C., Tsang, T., Gao, F., Li, X., Muller, J. P., Lewis, P. and Barnsley, M., (1999). *MODIS BRDF/Albedo Product: Algorithm Theoretical Basis Document Version 5.0,* 53 p. https://lpdaac.usgs.gov/documents/97/MCD43_ATBD.pdf. [ Accessed on October 2021].

Sunny, D.S., Islam, K.M.A., Mullick, M.R.A. and Ellis, J.T. (2022). Performance study of imageries from MODIS, Landsat 8 and Sentinel-2 on measuring shoreline change at regional scale. *Remote Sensing Applications: Society and Environment* **28**. https://doi.org/10.1016/j.rsase.2022.100816.

Swapna, P., Sreeraj, P., Sandeep, N., Jyoti, J., Krishnan, R., Prajeesh, A.G., Ayantika, D.C. and Manmeet, S. (2022). Increasing frequency of extremely severe cyclonic storms in the north Indian ocean by anthropogenic warming and southwest monsoon weakening. *Geophysical Research Letters* **49**(3). https://doi.org/10.1029/2021GL094650.

Szabo, S., Brondizio, E., Renaud, F.G., Hetrick, S., Nicholls, R.J., Matthews, Z., Tessler, Z., Tejedor, A., Sebesvari, Z., Foufoula-Georgiou, E., da Costa, S. and Dearing, J.A. (2016). Population dynamics, delta vulnerability and environmental change: Comparison of the Mekong, Ganges-Brahmaputra and Amazon delta regions. *Sustainability Science* **11**(4): 539-554. https://doi.org/10.1007/s11625-016-0372-6.

Wang, G.J., Garcia, D., Liu, Y., de Jeu, R. and Dolman, A.J. (2012). A three-dimensional gap filling method for large geophysical datasets: Application to global satellite soil moisture observations. *Environmental Modelling and Software* **30**: 139-142. https://doi.org/10.1016/j.envsoft.2011.10.015.

Welsch, C., Swenson, H., Cota, S.A., DeLuccia, F., Haas, J.M., Schueler, C., Durham, R.M., Clement, J.E. and Ardanuy, P.E. (2001). VIIRS (Visible Infrared Imager Radiometer Suite): A next-generation operational environmental sensor, Proceedings International Geoscience and Remote Sensing Symposium on *Scanning the present and resolving the future,* Vols 1-7, July 9-13, 2001, University of New South Wales, Sydney, Ausralia. pp 1020-1022. https://ieeexplore.ieee.org/document/976733.

Wulder, M.A., White, J.C., Loveland, T.R., Woodcock, C.E., Belward, A.S., Cohen, W.B., Fosnight, E.A., Shaw, J., Masek, J.G. and Roy, D.P. (2016). The global Landsat archive: Status, consolidation, and direction. *Remote Sensing of Environment* **185**: 271-283. https://doi.org/10.1016/j.rse.2015.11.032.